# Electrophysiological Properties Under Heart Failure Conditions in a Human Ventricular Cell: A Modeling Study

Mohamed M. Elshrif[1], IEEE Member, Pengcheng Shi[1], and Elizabeth M. Cherry[2]

***Abstract*— Heart failure (HF) is one of the major diseases across the world. During HF the electrophysiology of the failing heart is remodeled, which renders the heart more susceptible to ventricular arrhythmias. In this study, we quantitatively analyze the effects of electrophysiological remodeling of the major currents of human ventricular myocytes on the dynamics of the failing heart. We develop a HF model using a modified version of a recently published model of the human ventricular action potential, the O'Hara-Virág-Varró-Rudy (OVVR) model. The proposed HF model incorporates recently available HF clinical data. It can reproduce most of the action potential (AP) properties of failing myocytes, including action potential duration (APD), amplitude (APA), notch (APN), plateau (APP), resting membrane potential (RMP), and maximum upstroke velocity ($\mathbf{dV/dt_{max}}$). In addition, the model reproduces the behavior of the $[\mathbf{Na^+}]_\mathbf{i}$ concentration and $[\mathbf{Ca^{2+}}]_\mathbf{i}$ dynamics. Moreover, the HF model exhibits alternans with a fast pacing frequency and can induce early afterdepolarizations (EADs). Additionally, blocking the late sodium current shortens the APD and suppresses EADs, in agreement with experimental findings. The dynamics of the proposed model are assessed through investigating the rate dependence of the AP and the dynamics of the major currents. The steady-state (S-S) and S1-S2 restitution curves along with accommodation to an abrupt change in cycle length were evaluated. Our study should help to elucidate the roles of alterations in electrophysiological properties during HF. Also, this HF cellular model could be used to study HF in a realistic geometry and could be embedded into a model of HF electromechanics to investigate electrical and mechanical properties simultaneously during HF.**

## I. INTRODUCTION

Cardiovascular disease (CVD) is still the leading cause of morbidity and mortality in both developing and developed countries, [1], where the prevalence of CVD is $\sim$70% for people between 60-79 years. Mortality in the USA alone from cardiac diseases in 2010 is nearly 800,000 deaths, [1] with a significant number of these deaths caused by ventricular arrhythmia (VA). It is known that during HF cellular electrophysiology becomes altered and arrhythmia properties are changed. These alterations include ion channels [2] and intracellular calcium cycling [3]. Therefore, understanding VA mechanisms at the cellular level is critical.

In many cases, animal models are used to investigate cardiac electrophysiological properties for both control and HF cases. However, mathematical models and computer simulations also are important tools for studying arrhythmias. To study the mechanisms of VA in humans arising from HF, the mathematical model should be based on recent human data and reproduce important arrhythmogenic phenomena, such as the AP, $[Ca^{2+}]_i$ alternans, and EADs. Therefore, we develop a human ventricular cell model under HF conditions that is based on the OVVR model [4]. This physiologically-based mathematical model of a normal human ventricular cell was chosen because it is formulated to reproduce the normal human ventricular AP with a broad range of essential physiological properties, such as rate dependence and restitution curves of an APD, and because it is based on extensive experimental datasets. Furthermore, the model can reproduce alternans and EADs.

In our previous study [5], we performed a quantitative analysis of the OVVR model under normal conditions. In this manuscript, we develop a new HF model and quantitatively analyze its AP properties for different physiological cycle lengths (CLs) along with rate dependence properties associated with tachyarrhythmias, and we create APD restitution curves of APD. We investigate the important properties of alternans in the HF model and compare them with our previous findings using the original model [5]. In addition, our model has the ability to produce EADs, which is one of the main sources of VA [6]. Our simulation results show our model reproduces failing myocyte properties more closely than previous HF models [7], [8], which did not reproduce EADs and alternans. In addition, unlike in previous studies, we investigate the effect of rate dependence of the AP and the major currents, predict the behavior of the HF model using different pacing protocols, and assess short-term memory.

## II. METHODS

Our mathematical model of the HF-remodeled human ventricular action potential is based on data available in the literature describing specific cellular electrophysiological remodeling during human HF. The model can be described by the following differential equation.

$$dV_m/dt = -(1/C_m)(I_{Na} + I_{NaL} + I_{CaL} + I_{to} + I_{CaNa} + I_{CaK} + I_{Kr} + I_{Ks} + I_{K1} + I_{NaCa} + I_{NaK} + I_{Nab} + I_{Kb} + I_{Cab} + I_{pCa} + I_{stim}) \quad (1)$$

Here $V_m$ is the transmembrane potential, $t$ is time, $C_m$ is the membrane capacitance, and $I_{stim}$ is the stimulus current.

Research is supported by the Libyan-North American Scholarship Program from the Ministry of Higher Education, Scientific Research in Libya, the Ph.D. Program in Computing and Information Sciences at RIT, and the National Science Foundation under Grant Number CMMI-1028261.

[1]M. M. E. and P. S. are with the B. Thomas Golisano College of Computing and Information Sciences, Rochester Institute of Technology, Rochester, New York, USA. mme4362@rit.edu, spcast@rit.edu

[2]E. M. C. is with the School of Mathematical Sciences, Rochester Institute of Technology, Rochester, New York, USA. excsma@rit.edu

978-1-4244-7929-0/14/$26.00 ©2014 IEEE

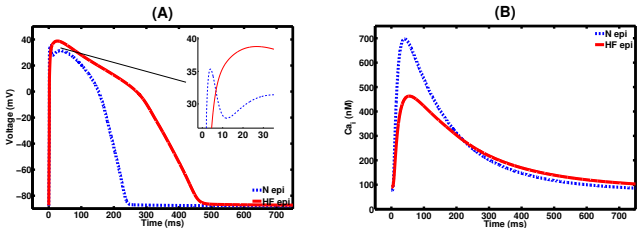


Fig. 1. Simulation of the epicardial OVVR model under normal (dotted blue) and HF (solid red) conditions. (A) AP. (B) $[Ca^{2+}]_i$ dynamics.

Under HF conditions, many of these ionic currents are altered; such alterations have been studied extensively in experiments [2], [3], [9], [10], [11], [12], [13], [14], and ultimately remodel an AP as well as $[Ca^{2+}]_i$ dynamics (see Fig. 1). We explain the alterations we adopted in each of the main altered ionic currents separately based on experimental studies; see Table 1.

- Fast Sodium Current ($I_{Na}$): This current is responsible for the initiation of normal impulses in a single cell. Most experimental studies on HF-affected myocytes indicate that the peak $I_{Na}$ current is decreased by 32% to 91% [9].
- Late Sodium Current ($I_{NaL}$): This slow current is active during the plateau and repolarization phases of an AP. Most experimental data on human myocytes show that the $I_{NaL}$ current density is increased by 30% to 238% during HF conditions [9], [15].
- L-type Calcium Current ($I_{CaL}$): This current is active during the AP plateau and repolarization, HF-induced remodeling of $I_{CaL}$ is controversial, with qualitatively different experimental observations. However, the majority of studies report that $I_{CaL}$ current does not change [14], [16].
- Transient Outward Potassium Current ($I_{to}$): This current affects the notch of the AP and is important in early repolarization. Most experiments on human cells report that $I_{to}$ current density is decreased between 26% and 75% under HF conditions [10], [16].
- Inward Rectifier Potassium Current ($I_{K1}$): This current is important in maintaining RMP and in the terminal repolarization phase of the AP. Experiments indicate that $I_{K1}$ current density is significantly downregulated by 40% to 64% [11], [16].
- Rapid Delayed Rectifier Potassium Current ($I_{Kr}$): This current plays a significant role during late repolarization of an AP. The modulation of this current in HF-remodeled myocytes has been studied extensively, but with varying results. However, most studies indicate that $I_{Kr}$ current density is reduced by 27% to 57% [11], [12].
- Slow Delayed Rectifier Potassium Current ($I_{Ks}$): This current affects an AP during late repolarization. Most studies on human and animal species under HF conditions show downregulation of $I_{Ks}$ current density by 50% to 60% [11], [16].

TABLE I
SUMMARY OF THE REMODELED CURRENTS OF THE HEART FAILURE OVVR MODEL IN A SINGLE EPICARDIAL CELL.

| **Current** | Heart Failure | Experimental Observations | References |
|---|---|---|---|
| $I_{Na}$ | ↓(57%) | ↓(32%-91%) | [9] |
| $I_{NaL}$ | ↑(200%) | ↑(30%-238%) | [9], [15] |
| $I_{CaL}$ | unchanged | unchanged | [14], [16] |
| $I_{to}$ | ↓(73%) | ↓(26%-75%) | [10], [16] |
| $I_{K1}$ | ↓(50%) | ↓(40%-64%) | [11], [16] |
| $I_{Kr}$ | ↓(45%) | ↓(27%-57%) | [11], [12] |
| $I_{Ks}$ | ↓(57%) | ↓(50%- 62%) | [11], [16] |
| $I_{NaCa}$ | ↑(200%) | ↑(50%-500%) | [13], [17] |
| $I_{NaK}$ | ↓(42%) | ↓(15%-45%) | [14] |
| $SERCA$ | ↓(25%) | ↓(25%-50%) | [18] |

- Sodium Calcium Exchanger Current ($I_{NaCa}$): $I_{NaCa}$ helps to regulate intracellular $Ca^{2+}$ and it is affected by the $[Ca^{2+}]_i$ and $[Na^{+}]_i$ concentrations as well as the transmembrane potential, all of which are modified during HF. Thus, an alteration in the $I_{NaCa}$ function will contribute to the abnormal regulation of $[Ca^{2+}]_i$ and $[Na^{+}]_i$ concentrations. Previous studies have found that the activity of the $I_{NaCa}$ is increased between 50% and 500% [13], [17].
- Sodium Potassium Exchanger Current ($I_{NaK}$): The $Na^{+}/K^{+}$ exchanger plays an important role in maintaining ionic homeostasis within the cell and stabilizing the RMP. The majority of experimental studies report that the $I_{NaK}$ activity is downregulated by between 15% and 45% in failing myocytes [14].
- Sarcoplasmic Reticulum $Ca^{2+}$ ($SERCA$): Its main function is to pump $Ca^{2+}$ ions from the cytosol into the SR. Ref. [18] reports an alteration of the $[Ca^{2+}]_i$ concentration in failing myocytes based on the dynamics of the SR $Ca^{2+}$ and indicates that the SERCA current is decreased by 25%.

### A. *Measurement of restitution curves and accommodation:*

To study the effects of CL perturbations on ventricular APD, three protocols used: steady-state restitution (S-S), S1-S2 restitution, and accommodation to a single change in cycle length. For each protocol, APs were generated by using a current strength twice diastolic threshold at a CL of 1s. APDs were measured using a repolarization voltage threshold of 50%, and 90% after pacing for 1min at the relevant CL. For the S-S protocol, the cell was stimulated for 1 min starting at a CL of 1s after which the CL was decreased monotonically until 2:1 block was observed. At each CL, the last APD and the prior diastolic interval (DI) pair were registered (during alternans, the last two DI, APD pairs were recorded). For the S1-S2 protocol, the cell was stimulated for 1 min with a fixed CL, which is represented as S1, after which a subsequent stimulation (S2) was used after a variable DI. The last values for DI and APD were measured. The memory amplitude was calculated as the difference in APD for the longest DI between the longest S1 CL (here,

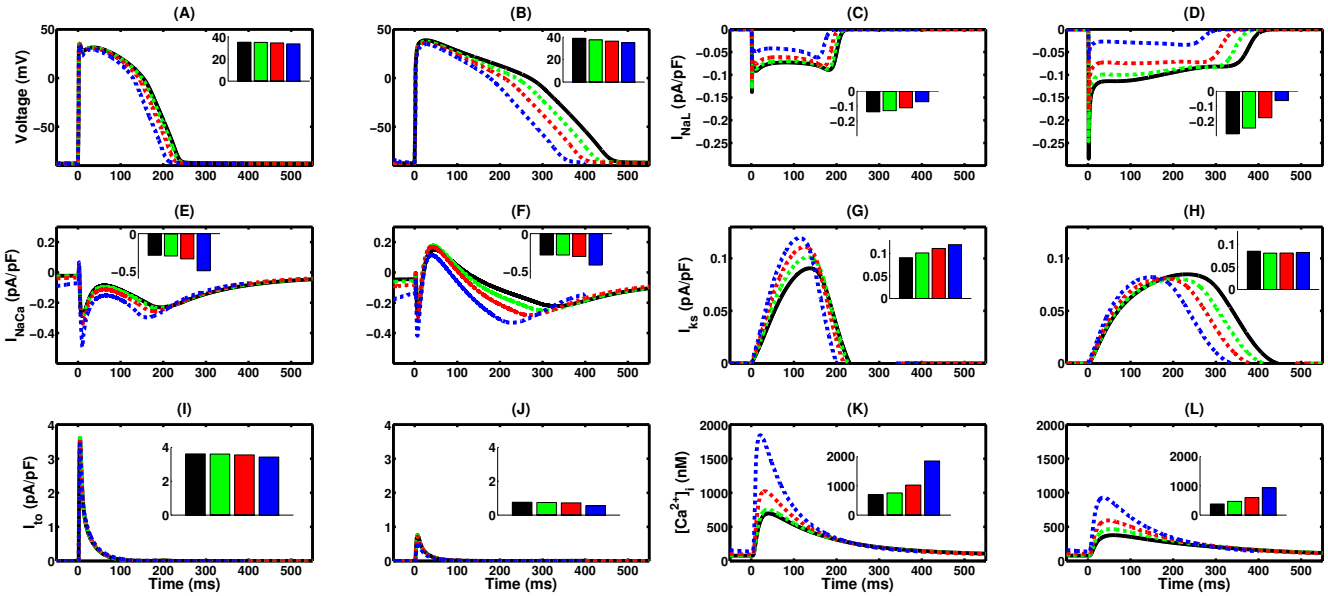


Fig. 2. Rate dependence of action potentials, primary transmembrane currents, and intracellular calcium concentration in a single myocyte for the normal (columns 1 and 3) and HF (columns 2 and 4) models for cycle lengths of 1000 ms (solid black), 800 ms (dashed green), 600 ms (dashed red), and 400 ms (dashed blue). The HF OVVR model generally shows more rate dependence; however, the normal OVVR model shows greater rate dependence for $I_{Ks}$ and $[Ca^{2+}]_i$.

1 s), and the shortest S1 CL before conduction block or alternans was observed [19]. Finally, we used a protocol measuring accommodation to a change in CL because it has been proposed as a clinical marker for arrhythmia risk [20]. Following previous studies [21], [22], the accommodation curve was constructed by measuring $APD_{90}$ at an initial CL of 1s after pacing for 8 min, after abruptly decreasing the CL to 600 ms for 8 min, and after restoring the CL to 1 s for 8 min. Since it is not always possible to reach a stable steady state using models, we paced the model with a constant CL for 5 min, after which the difference between consecutive APDs was found to be on the order of $10^{-4}$ ms.

### *B. Numerical Methods:*

The explicit Euler method was used to integrate our HF OVVR model with uniform time resolution. To integrate the ionic gating variables in the HF OVVR model; the Rush and Larsen method [23], was implemented. The temporal resolution used for the HF OVVR model was 0.02 ms, with the $[Ca^{2+}]$ equations integrated with a smaller time step of 0.001 ms. All single-variable functions were pre-computed and saved in lookup tables [24]. Initial conditions were set as in the normal OVVR model [4].

## III. RESULTS

### *A. HF Simulation of an AP in an Epicardial Cell:*

The simulated AP generates an AP in good agreement with what has been observed experimentally [25], as shown in Fig. 1-A, as well as the calcium transient, as depicted in Fig. 1-B. Table 2 summarizes the differences in quantitative biomarkers between the normal and HF models, along with observed values of these biomarkers from experiments when known.

### *B. Rate dependence of APD and Major Currents:*

As shown in Fig. 2A-B, APs of the HF model have a stronger dependence on rate than those of the normal model. Both models display low rate dependence of the $I_{NaL}$ current (see Fig. 2C-D); however, the maximum value of the $I_{NaL}$ current at small CLs (high pacing rates) in the HF model becomes less than that of the normal model. $I_{NaCa}$ exhibits rate dependence for both models with a larger degree for the normal model, as shown in Fig. 2E-F. The $I_{Ks}$ current under normal conditions is larger than the $I_{Ks}$ current under HF conditions by 10% (see Fig. 2G-H). The HF model shows almost no rate dependence of $I_{Ks}$ with only a slight decrease in the peak current value as CL is decreased. In contrast, peak $I_{Ks}$ increases as CL decreases for the normal model. For $I_{to}$, both models exhibit limited rate dependence, as shown in Fig. 2I-J, with a larger dependence in the HF model. Fig. 2K-L show that for both models the maximum value of $[Ca^{2+}]_i$ increases as the CL decreases from 1000 ms to 300 ms, which means that the peak-frequency relationship of the $[Ca^{2+}]_i$ concentration is positive for all CLs tested. In addition, the $[Ca^{2+}]_i$ curves rise and fall more rapidly for the original model than for the HF model.

Both models display limited rate dependence of $I_{CaL}$ (not shown). However, its maximum value for all CLs is more than double for the HF model compared to the normal model. $I_{K1}$ has similar patterns for both models; but, the maximum value of $I_{K1}$ in the HF model is $\sim$100% larger than that of the normal model (not shown). Both models show a small dependence of $I_{Kr}$ on rate; however, its maximum value for the normal model is two times larger than that for the HF model, suggesting that the reduction in this current contributes to APD prolongation during HF (not shown).

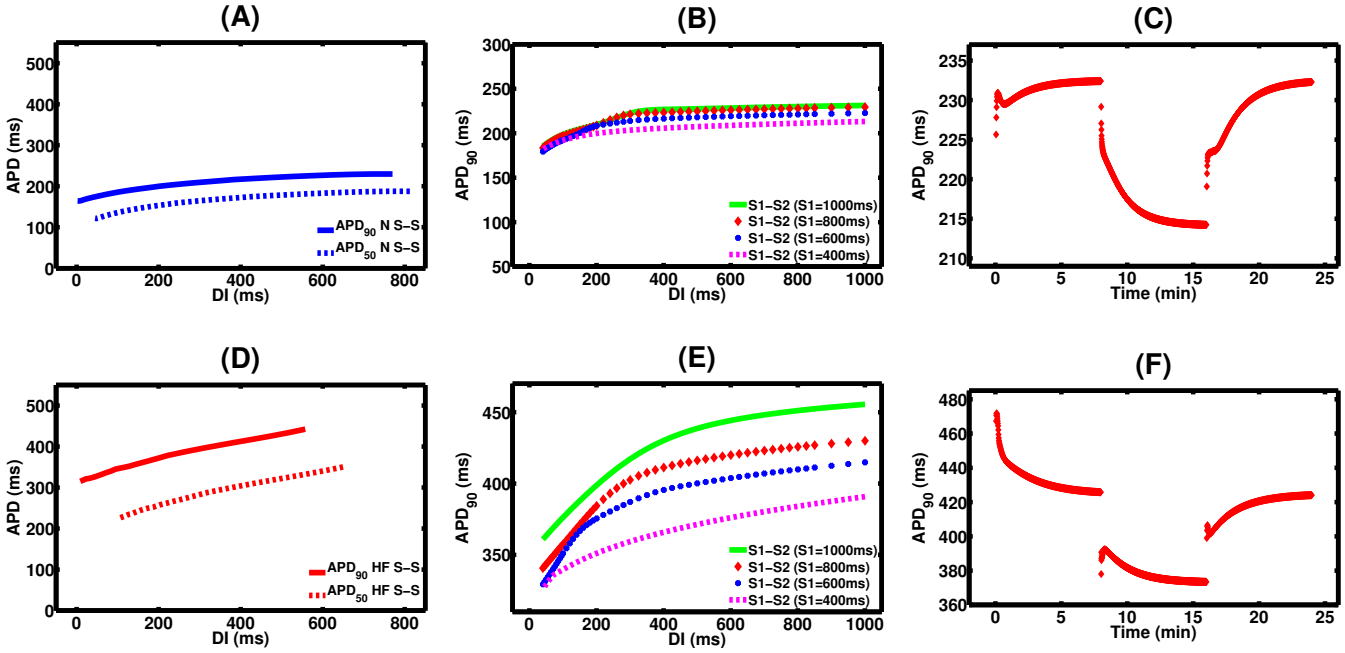


Fig. 3. Epicardial OVVR model restitution curves. S-S $APD_{90}$ and $APD_{50}$ restitution curves for (A) normal and (D) HF conditions. S1-S2 restitution curves for (B) normal and (E) HF conditions. Time course of APD accommodation after an abrupt decrease and abrupt increase in CL for the (C) normal and (F) HF cases.

### C. Restitution Curves and Short-term Memory:

Figure 3A-D shows S-S $APD_{50}$ and $APD_{90}$ restitution curves from both models. All S-S restitution curves decrease monotonically, with the HF model exhibiting a more marked decrease than the normal model. For all CLs that were less than 1s, APDs vary largely for the HF model (with a 127.4 ms decrease) compared to the normal model (with a 65.5 ms decrease). The effects of short-term memory (STM), which embodies the impact of the pacing history on the cell, can be quantified by calculating the difference in S1-S2 APD restitution curves as the S1 CL is changed. The STM values for the HF and normal models are 64.8 ms and 18.1 ms, respectively, as assessed using a CL of 1 s (see Fig. 3B-E). When accommodation to a decreased CL, the HF epicardial cell type first has a rapid decrease and increase in $APD_{90}$ followed by a slow decay to steady state. For the normal epicardial cell type, accommodation consists of a monotonic decrease to steady state. Similar behavior was observed for accommodation to an increased CL, as shown in Fig. 3C-F.

### D. Alternans:

For a normal myocyte, alternans occurs only for a CL of 165 ms, with a magnitude of 1.48 ms, as shown in Fig. 4A. In a failing myocyte, alternans occurs at higher CLs and for an extended alternans range of CLs between 460 and 320 ms, as shown in Fig. 4B. The magnitude is increased as well to 8.0 ms. Thus, alternans is obtained more easily under HF conditions.

### E. Inducing EADs in Epicardial Myocytes:

Ventricular arrhythmias and sudden cardiac death are often associated with HF [26], with early afterdepolarizations thought to play an important role in the initiation of arrhythmias. Therefore, it is important to reproduce EADs in our HF model. Our simulation results are in agreement with experimental observations [27], with $APD_{90}$ measurement of 1247.0 ms for simulated epicardial HF cells compared to experimental observations in LQT2 myocytes of 1292.1±189.5 ms for a CL 4000 ms in both cases, (see Fig. 4A). Additionally, blocking the $I_{NaL}$ current in our HF model shortens APs and suppresses EADs, in agreement with experimental observations [28].

TABLE II
ELECTROPHYSIOLOGICAL PROPERTIES IN NORMAL AND HF-REMODELED EPICARDIAL CELLS.

| Metric | Normal Simulation | Heart Failure Simulation | Experimental Observations |
|---|---|---|---|
| $APD_{90}$ (ms) | 229.0 | 440.8 | [29] |
| $APD_{50}$ (ms) | 182.0 | 337.5 | [29] |
| $Triangulation$ (ms) | 47.0 | 103.3 | [7], [30] |
| $RMP$ (mV) | -87.8 | -87.4 | [31] |
| $Amplitude$ (mV) | 123.1 | 111.2 | - |
| $V_{notch}$ (mV) | 27.8 | 28.6 | - |
| $V_{plateau}$ (mV) | 31.4 | 38.8 | - |
| $dV/dt_{max}$ (V/s) | 217.1 | 113.6 | - |
| $STM$ (ms) | 18.1 | 64.8 | - |
| $CL_{min}$ (ms) | 165.0 | 320.0 | - |
| S-S $Max.\ slope$ | 0.36 | 0.47 | - |
| $Alternans\ onset\ CL$ | 165.0 | 460.0 | [34], [35] |
| $[Ca^{2+}]_i$ SA (nM) | 697.5 | 378.4 | [7], [30] |
| $[Ca^{2+}]_i$ TT (ms) | 40.9 | 59.7 | [7], [30], [32] |
| $[Na^{+}]_i\ peak$ (ms) | 9.1 | 10.2 | [33] |

## IV. DISCUSSION AND CONCLUSION

In this manuscript, we present a model of human heart failure based on remodeling ion channels and transporters in the OVVR model to reproduce the AP properties of failing

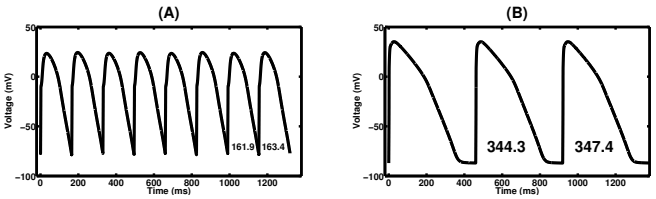


Fig. 4. Alternans in a single epicardial cell from the OVVR model. (A) AP traces for a normal cell. (B) AP traces for a HF cell.

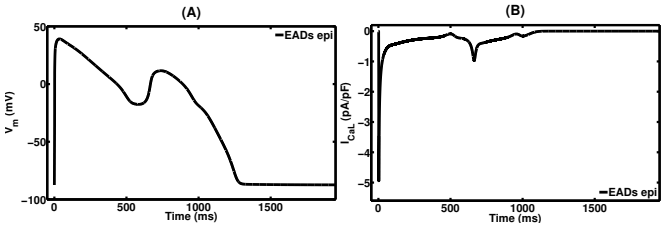


Fig. 5. Early afterdepolarizations (EADs) in an epicardial cell for the OVVR HF model. (A) AP. (B) Corresponding $I_{CaL}$ current.

human myocytes. We have compared our model's properties with available experimental and clinical observations and find good agreement, as shown in Table 2. We find that $APD_{90}$ is prolonged by 211.8 ms in our model, which agrees with experimental observations of $\sim$181$\pm$28 ms prolongation for the HF case [29]. In addition, we find that $APD_{50}$ is prolonged by 155.5 ms during HF, similar to experimental findings of $\sim$156$\pm$22 ms at a CL of 2000 ms [29].

Under HF conditions, triangulation, which is the difference between $APD_{90}$ and $APD_{50}$, was comparable between our simulations (56.25 ms) and experimental studies [7], [30]. Experiments also showed a slight increase in RMP ranging from 0.2 to 1.0 ms [31], which is in agreement with the 0.38 ms in our model. In addition, properties of the simulated $Ca^{2+}$ transient match experimental findings, including decreased systolic amplitude (SA) ($\downarrow$46% in our model compared to $\downarrow$41% in experiments [30] and [17]) and a slight increase in diastolic $[Ca^{2+}]_i$ [30]. The difference between the systolic amplitude of $[Ca^{2+}]_i$ in HF and normal cells has been observed to be 379$\pm$140 nM [30], which is in the range of the difference observed for our model of 296 nM. The difference of the upstroke time or time to peak (TT) for the $Ca^{2+}$ transient is 20$\pm$11 ms for a CL of 3000 ms [32], whereas in our model it is 18.8 ms. The $[Na^{+}]_i$ concentration is increased in HF cells for all stimulation rates when compared with the normal cell, which matches the previous results [33].

Our model includes some limitations. Recent work on mRNA [34] has shown that alternans in human HF cells begins at a CL of 350 ms, whereas alternans in our case is higher by 110 ms. However, it is close to the observed value reported in other studies [35] of $\leq$500 ms. In additional, in our simulation results, we observe that the maximum APD S-S restitution curve slope is 0.47, which is less than the slope value of 0.86$\pm$0.12 measured in the LV free wall of the failing human heart [3]. This difference may be due to electronic effects.

In comparing our model with previous HF simulation models [7], [8], we found that these models did not reproduce as many of the properties of HF that are observed in a single human HF-remodeled myocyte, such as leveraged accumulated $[Na^{+}]_i$ concentration, alternans, and EADs. These models were designed to reproduce the two prominent properties: prolonged $APD_{90}$ and altered $[Ca^{2+}]_i$ dynamics. Also, these studies used more limited data and did not show most of the HF-remodeled properties in a quantitative manner. Most of the previous models, [7], [8], did not consider remodeling the $I_{Na}$ current in reproducing the reduction in the upstroke velocity of HF cells. Also, these models either did not remodel the $I_{NaL}$ current [7] or exaggerated its increase [8]. Moreover, previous simulation studies did not incorporate remodeling of $I_{to}$ and $I_{Kr}$ currents. Previous simulation studies, [7], [8] did not change these currents.

We have shown that our model is not only accurate in reproducing $APD_{90}$, $APD_{50}$, and $[Ca^{2+}]_i$ dynamics, but also that it can replicate the behavior of $[Na^{+}]_i$ observed in human failing myocytes along with increased AP triangulation, which is a harbinger for cardiac arrhythmias. Also, the dynamical behavior of the HF model was quantified using different protocols. In future work, we intend to study our model's properties in tissue, including conduction velocity (CV), and to determine how HF remodeling at the cellular level affects the spatiotemporal dynamics of induced arrhythmias in realistic heart geometries. Also, the inclusion of CaMK in the model will facilitate examining how drug-induced alterations in ionic current properties could modulate the electrophysiological properties in HF.

## REFERENCES


[1] Go AS, et al. Heart disease and stroke statistics-2014 update: a report from the American Heart Association. Circ. 2014.

[2] Soltysinska E, et al. Transmural expression of ion channels and transporters in human nondiseased and end-stage failing hearts. Pflugers Arch.459:11-23, 2009.

[3] Glukhov AV, et al. Transmural dispersion of repolarization in failing and nonfailing human ventricle. Circ. Res. 106: 981-991, 2010.

[4] Thomas O'Hara, László Virág, András Varró, and Yoram Rudy. Simulation of the undiseased human cardiac ventricular action potential: Model formulation and experimental validation. PLoS Comput Biol, 7(5):e1002061, 05 2011.

[5] Elshrif, Mohamed M., and Cherry, Elizabeth M., A Quantitative Comparison of the Behavior of Human Ventricular Cardiac Electrophysiology Models in Tissue. PLoS ONE, 9: e84401, 2014.

[6] M.J. Janse, Electrophysiological changes in heart failure and their relationship to arrhythmogenesis. Cardiovasc Res 61: 208-217, 2004.

[7] Leo Priebe and Dirk J. Beuckelmann. Simulation study of cellular electric properties in heart failure. Circ. Res., 82(11):1206 -1223, 98.

[8] Yunliang Zang and Ling Xia. Electrical remolding and mechanical changes in heart failure: A model study. volume 6330 of Lecture Notes in Computer Science, pages 421-429, 2010.

[9] Carmen R. Valdivia, William W. Chu, Jielin Pu, Jason D. Foell, Robert A. Haworth, Mathew R. Wolff, Timothy J. Kamp, and Jonathan C. Makielski. Increased late sodium current in myocytes from a canine heart failure model and from failing human heart. Journal of Molecular and Cellular Cardiology, 38(3): 475-483, 2005.

[10] Stephen Zicha, Ling Xiao, Sara Stafford, Tae Joon Cha, Wei Han, Andras Varro, and Stanley Nattel. Transmural expression of transient outward potassium current subunits in normal and failing canine and human hearts. The Journal of Physiology, 561(3):735-748, 2004.

[11] Fadi G. Akar, Richard C. Wu, George J. Juang, Yanli Tian, Mirka Burysek, Deborah DiSilvestre, Wei Xiong, Antonis A. Armoundas, and Gordon F. Tomaselli. Molecular mechanisms underlying $K^+$ current down-regulation in canine tachycardia-induced heart failure. American Journal of Physiology - Heart and Circulatory Physiology, 288(6):H2887-H2896, 2005.

[12] Katherine M. Holzem Alexey V. Glukhov Igor R. Efimov. The role of $I_{Kr}$ in transmural repolarization abnormalities in human heart failure. Circulation, 124(A16014), 2011.

[13] Ion A. Hobai and Brian O'Rourke. Enhanced $Ca^{2+}$-activated $Na^+/Ca^{2+}$ exchange activity in canine pacing-induced heart failure. Circulation Research, 87(8):690-698, 2000.

[14] Robert H. G. Schwinger, Jiangnan Wang, Konrad Frank, Jochen Mller- Ehmsen, Klara Brixius, Alicia A. McDonough, and Erland Erdmann. Reduced sodium pump 1, 3, and 1-isoform protein levels and $Na^+/K^+$-ATPase activity but unchanged $Na^+/Ca^{2+}$ exchanger protein levels in human heart failure. Circulation, 99(16):2105-2112, 1999.

[15] Victor A. Maltsev, Norman Silverman, Hani N. Sabbah, and Albertas I. Undrovinas. Chronic heart failure slows late sodium current in human and canine ventricular myocytes: Implications for repolarization variability. European Journal of Heart Failure, 9(3):219-227, 2007.

[16] Gui-Rong Li, Chu-Pak Lau, Tack-Ki Leung, and Stanley Nattel. Ionic current abnormalities associated with prolonged action potentials in cardiomyocytes from diseased human right ventricles. Heart Rhythm, 1(4):460 - 468, 2004.

[17] Weber CR,Piacentino VIII,Houser SR,Bers DM. Dynamic regulation of $Na^+/Ca2+$ exchange function in human heart failure. Circulation 108:222429, 2003.

[18] Ming Tao Jiang, Andrew J. Lokuta, Emily F. Farrell, Matthew R. Wolff, Robert A. Haworth, and Hctor H. Valdivia. Abnormal ca2+ release, but normal ryanodine receptors, in canine and human heart failure. Circulation Research, 91(11):1015-1022, 2002.

[19] Cherry EM, Fenton FH (2007) A tale of two dogs: analyzing two models of canine ventricular electrophysiology. Am J Physiol Heart Circ Physiol 292: H43-55. doi:00955.2006.

[20] E. Pueyo, P. Smetana, P. Caminal, A. Bayes de Luna, M. Malik, and P. La- guna. Characterization of qt interval adaptation to rr interval changes and its use as a risk-stratifier of arrhythmic mortality in amiodarone-treated survivors of acute myocardial infarction. Biomedical Engineering, IEEE Transactions on, 51(9):1511-1520, Sept 2004.

[21] Chu Pak Lau, Andrew R. Freedman, Simon Fleming, Markek Malik, A. John Canm, and David E. Ward. Hysteresis of the ventricular paced qt interval in response to abrupt changes in pacing rate. Cardiovascular Research, 22(1):67-72, 1988

[22] M. R. Franz, C. D. Swerdlow, L. B. Liem, and J. Schaefer. Cycle length dependence of human action potential duration in vivo. effects of single extrastimuli, sudden sustained rate acceleration and deceleration, and different steady-state frequencies. The Journal of Clinical Investigation, 82(3):972979, 9 1988.

[23] Rush S., and Larsen H., A practical algorithm for solving dynamic membrane equations. IEEE Trans Biomed Eng 25: 389392, 1978.

[24] Hodgkin AL., Huxley AF., A quantitative description of membrane currents and its application to conduction and excitation in nerve. J Physiol 117:500544, 1952.

[25] Gui-Rong Li, Chu-Pak Lau, Anique Ducharme, Jean-Claude Tardif, and Stanley Nattel. Transmural action potential and ionic current remodeling in ventricles of failing canine hearts. American Journal of Physiology - Heart and Circ. Physio., 283(3):H1031-H1041, 2002.

[26] Gorgels AP Vos MA Smeets JL and Wellens HJ. Ventricular arrhythmias in heart failure. Am J Cardiol., 70(10):37C43C, 1992

[27] Gong-Xin Liu, Bum-Rak Choi, Ohad Ziv, Weiyan Li, Enno de Lange, Zhilin Qu, and Gideon Koren. Differential conditions for early afterdepolarizations and triggered activity in cardiomyocytes derived from transgenic LQT1 and LQT2 rabbits. The Journal of Physiology, 590(5):11711180, 2012.

[28] A. I. Undrovinas, V. A. Maltsev, and H. N. Sabbah. Repolarization abnormalities in cardiomyocytes of dogs with chronic heart failure: role of sustained inward current. Cellular and Molecular Life Sciences CMLS, 55:494505, 1999.

[29] Li G, Lau C, Leung T, Nattel S, Ionic current abnormalities associated with prolonged action potentials in cardiomyocytes from diseased human right ventricles. Heart Rhythm 4: 460-468, 2004.

[30] D. J. Beuckelmann, M. Nbauer, and E. Erdmann. Intracellular calcium handling in isolated ventricular myocytes from patients with terminal heart failure. Circulation, 85(3):104655, 1992.

[31] Yuri A. Kuryshev, Gary M. Brittenham, Hisashi Fujioka, Perry Kannan, Char-Chang Shieh, Sidney A. Cohen, and Arthur M. Brown. Decreased sodium and increased transient outward potassium currents in iron-loaded cardiac myocytes: Implications for the arrhythmogenesis of human siderotic heart disease. Circulation, 100(6):675683, 1999.

[32] Gwathmey G, Copelas L, MacKinnon R, Schoen F, Feldman M, et al. Abnormal intracellular calcium handling in myocardium from patients with end-stage heart failure. Circ Res 61: 70-76, 1987.

[33] DM. Bers. Excitation-Contraction Coupling and Cardiac Contractile Force. Kluwer Academic, Netherlands, Dordrecht, 2001.

[34] Walmsley J, et al. mRNA expression levels in failing human hearts predict cellular electrophysiological remodeling: A population-based simulation study. PLoS ONE 8(2):e56359, 2013.

[35] Wilson LD, Jeyaraj D, Wan X, Hoeker GS, Said TH, Gittinger M, Laurita KR, Rosenbaum DS. Heart failure enhances susceptibility to arrhythmogenic cardiac alternans. Heart Rhythm. 6:251259, 2009.